

# Second-order cone programming with probabilistic regularization for robust adaptive beamforming

Xijing Guo<sup>a)</sup>

Key Laboratory of Ocean Acoustics and Sensing (Northwestern Polytechnical University),  
Ministry of Industry and Information Technology, Xi'an 710072, China  
[xguo@nwpu.edu.cn](mailto:xguo@nwpu.edu.cn)

Sebastian Miron

Université de Lorraine, Centre de Recherche en Automatique de Nancy, Unité Mixte de  
Recherche 7039, Vandœuvre-lès-Nancy, F-54506, France  
[sebastian.miron@univ-lorraine.fr](mailto:sebastian.miron@univ-lorraine.fr)

Yixin Yang<sup>a),b)</sup>

Key Laboratory of Ocean Acoustics and Sensing (Northwestern Polytechnical University),  
Ministry of Industry and Information Technology, Xi'an 710072, China  
[yxyang@nwpu.edu.cn](mailto:yxyang@nwpu.edu.cn)

Shi'e Yang<sup>a)</sup>

College of Underwater Acoustic Engineering, Harbin Engineering University,  
145 Nantong Street, 150001 Harbin, China  
[yangshie@hrbeu.edu.cn](mailto:yangshie@hrbeu.edu.cn)

**Abstract:** Probabilistic regularization (PR) is introduced to make superdirective array beamforming robust against sensor characteristic mismatches. The objective is to enlarge the directivity while ensuring robustness with high probability. The PR problem is solved via the second-order cone programming where the regularization parameter is chosen through a statistical analysis of the system perturbations, based on Monte Carlo simulations. Experiments are carried out on a miniaturized  $3 \times 3$  uniform rectangular array without calibration. The results show that for this particular array, the PR method is robust to sensor mismatches and achieves a higher level of directivity compared with other robust adaptive beamforming approaches.

© 2017 Acoustical Society of America  
[TDM]

**Date Received:** December 5, 2016    **Date Accepted:** January 19, 2017

## 1. Introduction

Superdirective beamforming is sensitive to the distortions of the sensor characteristics, i.e., the sensor gain, phase, and position. Array calibration can be used in practice to alleviate the adverse effects caused by sensor mismatches. However, for underwater applications, especially at low frequencies, high-quality calibration is difficult to achieve because an anechoic laboratory environment is generally unavailable. Hence, robust beamforming approaches are required to remedy this situation.

Many robust data-independent beamforming approaches have already been proposed in array processing literature. In Refs. 1 and 2, the sensor characteristic mismatch problem is tackled using redundant sensors, whereas in Ref. 3 robustness is achieved using only the low-order “eigenbeams” for pattern synthesis. A weighted least squares (WLS) method was introduced,<sup>4</sup> which minimizes, from a statistical perspective, the mean deviation of the actual beam pattern from the desired one. This WLS approach was further generalized<sup>5</sup> by fully exploiting the degrees of freedom in the weighting functions, and solved by the Tikhonov regularization. For the WLS approach, the expectations are evaluated by integrations over a multidimensional grid, which can be extremely large and computationally expensive. In Ref. 6, the statistical analysis on the impact of the sensor mismatches is carried out using the more computationally efficient Monte Carlo (MC) simulation. Therein, the regularization parameter that governs the tradeoff between directivity and robustness is determined by maximizing from the statistical perspective some performance measure such as the

<sup>a)</sup>Also at: School of Marine Science and Technology, Northwestern Polytechnical University, Xi'an 710072, China.

<sup>b)</sup>Author to whom correspondence should be addressed.

directivity index (DI) or the front-to-back ratio. This strategy inspired the present work.

The *robust adaptive beamforming* was probably introduced by Cox *et al.*,<sup>7</sup> and is now more widely known as the diagonal loading (DL) approach. The DL imposes an extra white noise gain (WNG) constraint on the standard Capon beamforming, to ensure robustness against the sensor mismatches and can be efficiently solved via the second-order cone (SOC) programming.<sup>8</sup> The approach improves the robustness if an optimal selection of the DL level is made; however, in practice, the DL level is largely chosen in an *ad hoc* way due to the absence of a reliable rule. The general-linear-combination-based robust Capon beamformer,<sup>9</sup> i.e., the so-called GLC, and the midway method<sup>10</sup> are recent extensions of DL that can automatically determine the DL level.

Other extensions of DL also exist, e.g., the worst-case performance optimization proposed by Vorobyov *et al.*<sup>11</sup> However, to ensure robustness in the worst case, a very strong constraint is imposed, which negatively impacts the array directivity. We propose to use a looser probabilistic constraint, in order to achieve a good compromise between DI and robustness with high probability. Instead of directly solving this probabilistic regularization (PR) problem, we solve a SOC programming problem where the key is to determine an adequate regularization parameter. Several educated guesses of the regularization parameter are made and for each guess, MC simulations are carried out to test whether the probabilistic constraint holds in the presence of sensor mismatches. The guess that marginally passes this test is the desired regularization parameter and the corresponding beamformer weights provide the optimum solution via the SOC programming.

## 2. The proposed approach

Consider a miniaturized acoustic sensor array composed of  $L$  elements, deployed in the two-dimensional (2D) horizontal plane. In this plane, a narrowband plane wave  $s(k)$ , where  $k$  is the time index, of center (angular) frequency  $\omega$ , arrives from the azimuthal angle  $\phi$  with velocity  $c$ . The distance between any two adjacent sensors is much smaller than the wavelength  $\lambda = 2\pi c/\omega$ . The signal at the output of the sensor array can be expressed as an  $L \times 1$  vector

$$\mathbf{x}(k) = \mathbf{a}s(k) + \mathbf{n}(k), \quad (1)$$

where  $\mathbf{a}$  denotes the array manifold and  $\mathbf{n}(k)$  the noise vector. The  $\ell$ th element of  $\mathbf{a}$  is given by

$$a_\ell(\omega, \phi) = g_\ell e^{j\psi_\ell} e^{j\omega(x_\ell \cos \phi + y_\ell \sin \phi)/c}, \quad (2)$$

where  $g_\ell$  and  $\psi_\ell$  are the sensor gain and phase, respectively. It is worth mentioning that, in the ideal case where the sensors are all identical, the term  $g_\ell e^{j\psi_\ell}$  can be directly substituted with unity without loss of generality. The sensor position is determined by the 2D coordinates  $(x_\ell, y_\ell)$ .

The actual manifold vector  $\tilde{\mathbf{a}}$  lies in the  $\varepsilon$ -neighborhood of the nominal manifold vector  $\mathbf{a}$ , i.e.,  $\tilde{\mathbf{a}} \in \mathcal{U}(\mathbf{a}, \varepsilon)$ . Here, the distortion of  $\tilde{\mathbf{a}}$  from  $\mathbf{a}$  is measured by  $\delta = \|\tilde{\mathbf{a}} - \mathbf{a}\|_2$ , and  $\varepsilon$  sets the upper bound on  $\delta$ . The sensor mismatches will inevitably lead to a distorted beam pattern  $\mathcal{B}(\phi) = \mathbf{w}^H \tilde{\mathbf{a}}$ , where  $\mathbf{w}$  denotes the vector of the beamformer weights, and possibly cause a significant performance loss.

The worst-case performance optimization<sup>11</sup> provides a solution with high robustness against the sensor mismatches, expressed as

$$\min_{\mathbf{w}} \mathbf{w}^H \mathbf{R} \mathbf{w} \quad \text{subject to} \quad |\mathbf{w}^H \tilde{\mathbf{a}}| \geq 1, \quad \forall \tilde{\mathbf{a}} \in \mathcal{U}(\mathbf{a}, \varepsilon), \quad (3)$$

where

$$\mathbf{R} = \sum_{k=1}^K \mathbf{x}(k) \mathbf{x}^H(k)$$

is the sample covariance matrix and  $K$  is the training sample size. This problem is found equivalent to<sup>11</sup>

$$\begin{aligned} \min_{\mathbf{w}} \mathbf{w}^H \mathbf{R} \mathbf{w} \quad \text{subject to} \quad & \varepsilon \|\mathbf{w}\| \leq \mathbf{w}^H \mathbf{a} - 1, \\ & \Im(\mathbf{w}^H \mathbf{a}) = 0, \end{aligned} \quad (4)$$

where  $\Im(\cdot)$  denotes the imaginary part. This is a direct consequence of the triangle inequality:  $|\mathbf{w}^H \tilde{\mathbf{a}}| = |\mathbf{w}^H \mathbf{a} + \mathbf{w}^H (\tilde{\mathbf{a}} - \mathbf{a})| \geq |\mathbf{w}^H \mathbf{a}| - \|\mathbf{w}\| \|\tilde{\mathbf{a}} - \mathbf{a}\| \geq |\mathbf{w}^H \mathbf{a}| - \varepsilon \|\mathbf{w}\|$ . It is

obvious that the constraint of Eq. (3) holds, i.e.,  $|\mathbf{w}^H \tilde{\mathbf{a}}| \geq 1$ , if  $|\mathbf{w}^H \mathbf{a}| - \varepsilon \|\mathbf{w}\| \geq 1$ . Furthermore, if  $\Im(\mathbf{w}^H \mathbf{a}) = 0$ , then the condition  $|\mathbf{w}^H \mathbf{a}| - \varepsilon \|\mathbf{w}\| \geq 1$  reduces to  $\varepsilon \|\mathbf{w}\| \leq \mathbf{w}^H \mathbf{a} - 1$ , which is exactly the constraint of Eq. (4). Readers are referred to Ref. 11 for more details. Equation (4) expresses a SOC programming problem. Several sophisticated softwares, such as the MATLAB CVX toolbox,<sup>12</sup> are nowadays available to solve the SOC problem efficiently.

Observe that the constraint of Eq. (3) is a very strong condition, inclined to a high level of robustness, implying in return a directivity cutback. We propose a regularization approach, namely, the PR, to achieve higher directivity while ensuring robustness with an acceptable probability  $p$ ,

$$\min_{\mathbf{w}} \mathbf{w}^H \mathbf{R} \mathbf{w} \quad \text{subject to} \quad P(|\mathbf{w}^H \tilde{\mathbf{a}}| \geq 1) = p, \quad (5)$$

where  $P(\cdot)$  denotes the probability measure. For notational simplicity, we denote

$$\gamma = |\mathbf{w}^H \tilde{\mathbf{a}}|$$

in the subsequent discussions.

An explicit solution to this problem is not obvious. Alternatively, we solve the SOC programming [Eq. (4)] where the upper bound  $\varepsilon$  of the manifold distortion  $\delta$  is replaced by a smaller value  $\bar{\varepsilon}$  depending on a desired probability  $p$ . To estimate  $\bar{\varepsilon}$ , the statistics of the array perturbations in phase, amplitude, and position are needed; this information can be accessed via the sensor and the array manufacturers. Several guesses of  $\bar{\varepsilon}$  are made, with the initial guess around the mean of  $\delta$ . Then, the value of  $\bar{\varepsilon}$  is increased at each trial by a fraction/multiple of  $\delta$ 's standard deviation. The mean and the standard deviation of  $\delta$  are obtained by MC simulations, using the assumed probability density functions of the perturbations. Then, given a certain pre-specified probability  $p$ , trials are carried out based on MC simulation, to test whether the constraint of Eq. (5) is satisfied. The smallest value of  $\bar{\varepsilon}$  that satisfies this constraint is accepted.

A short summary of the proposed method is outlined hereafter:

- (1) Perform MC simulations to derive the mean  $\mu$  and the standard deviation  $\sigma$  of the distortion  $\delta$  of the actual manifold vector  $\tilde{\mathbf{a}}$  from the nominal manifold  $\mathbf{a}$ .
- (2) Make several guesses on  $\bar{\varepsilon}$  in terms of  $\mu$  and  $\sigma$ .
- (3) For each guess, run MC simulations, where statistical realizations of the sample covariance matrix  $\mathbf{R}$  in the presence of sensor characteristic perturbations and the guess of  $\bar{\varepsilon}$  are substituted in problem (4) to find the corresponding beamformer filter weights  $\mathbf{w}$  by the SOC programming. Accept the guess if the constraint of Eq. (5) is satisfied; otherwise, reject it.
- (4) Choose from the accepted guesses the smallest one to be  $\bar{\varepsilon}$ . Apply this  $\bar{\varepsilon}$  in the SOC problem (4) with the actual estimate of the covariance matrix  $\mathbf{R}$  to derive the beamformer weights, which provide the solution to the initial PR problem (5).

Notice that herein, MC simulations are carried in two different stages of the algorithm. MC simulation is first used to obtain the statistics of the array perturbations. Then, it is used to render the probability of  $\gamma \geq 1$ , in order to test the validity of the constraint of Eq. (5). Observe that in Ref. 6 MC simulation is only used to derive the statistics of a performance measure such as the DI or the front-to-back ratio.

### 3. Experiments

At Harbin Engineering University, a miniaturized  $3 \times 3$  uniform rectangular array (URA) has been built in order to test the performance of the proposed method. The inter-sensor spacing  $d$  is set to 0.12 m. In practice, perturbations exist in the sensor gains, phases, and positions. In this letter, these perturbations are assumed to be independent and identically distributed among the sensors, and follow Gaussian distributions. Specifically, for any  $\ell$  in between 1 and 9, the sensor gain  $g_\ell \sim N(1, 0.1)$  and the phase  $\psi_\ell \sim N(0^\circ, 10^\circ)$ . The sensor position perturbations are 2D random variables with equal standard deviations for both dimensions, which are 3% of the inter-sensor spacing  $d$ . The operating frequency is 300 Hz and the steering angle is  $0^\circ$ .

First, a statistical analysis is carried out to determine the value of the regularization parameter  $\bar{\varepsilon}$ . Figure 1(a) shows the histogram of  $\delta = \|\tilde{\mathbf{a}} - \mathbf{a}\|_2$ , obtained from  $10^6$  realizations of  $\tilde{\mathbf{a}}$ . Herein, the mean of  $\delta$  equals  $\mu = 0.518$  and the standard deviation  $\sigma = 0.119$ . The theoretical probability density function of the Gaussian distribution with the same statistics is also illustrated for comparison. It is obvious that  $\delta$  largely follows the Gaussian distribution  $N(\mu, \sigma)$ . Hence, if the regularization parameter

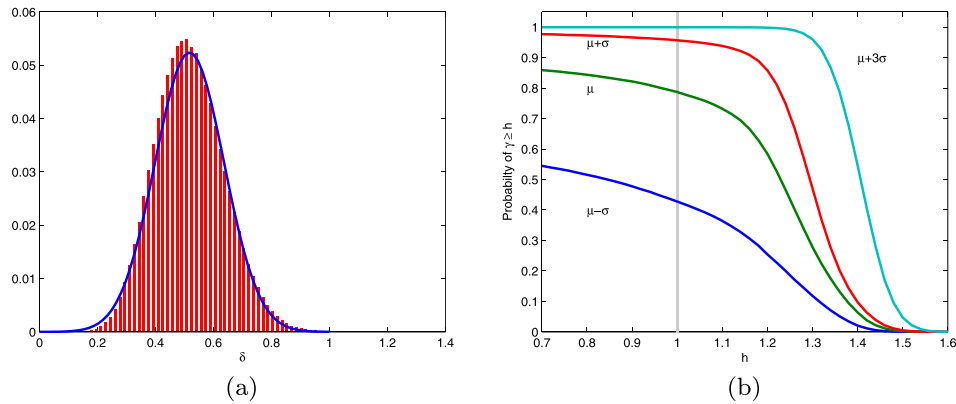


Fig. 1. (Color Online) (a) Histogram of  $\delta$  compared to the probability density function of the Gaussian distribution with the same mean and standard deviation (smooth curve). (b) Probabilities of  $\gamma$  to be greater than or equal to the abscissa, for different values of  $\bar{\epsilon}$ .

$\bar{\epsilon} = \mu + 3\sigma = 0.875$ , then  $\delta \leq \bar{\epsilon}$  with probability 99.85% at least. In this case,  $\bar{\epsilon} \approx \epsilon$ , i.e., the upper bound of  $\delta$ , and the PR problem reduces to the worst-case performance optimization.<sup>11</sup>

Once  $\bar{\epsilon}$  is determined, the weights  $\mathbf{w}$  can be sought via solving the SOC programming problem (4) with  $\epsilon$  substituted by  $\bar{\epsilon}$ . Then, we evaluate the chance that the constraint  $\gamma \geq 1$  is satisfied. Figure 1(b) shows the probabilities of  $\gamma \geq h$  with respect to a real nonnegative constant  $h$ , for four different guesses of  $\bar{\epsilon}$ . Forty thousand realizations are drawn to generate one such curve. The point with respect to  $h = 1$  indicates the probability of  $\gamma \geq 1$ , i.e.,  $p$  in the constraint of Eq. (5). The exact values of  $p$  for the four cases are tabulated in Table 1. Obviously, if

$$\mu \leq \bar{\epsilon} \leq \mu + \sigma$$

the constraint  $\gamma \geq 1$  is satisfied with a high probability of 79% to 96%.

In mid-November 2013, we carried out several experiments on Qiandao Lake (Zhejiang province, China). The sensor array was deployed horizontally in the water column. A sound source was placed in the far field of the array, transmitting rectangular continuous wave pulses with different carrier frequencies. The pulses were repeated every second and each pulse lasted 20 cycles in terms of the carrier frequency. To test the response of the array to all possible azimuthal incident angles, the array was rotated around its center in the horizontal plane. For each incident angle, 30 pulses were recorded. The dataset for 300 Hz, without calibration, is now used to examine the performance of the proposed method.

Figure 2(a) illustrates the measured beam patterns for three different values of the regularization parameter  $\bar{\epsilon}$ , where the main response axis of the array is steered at  $0^\circ$ . These beam patterns are generated as follows. For each incident angle, the squared amplitudes of the pulses at the beamformer output are averaged over the 30 pulses; the result is taken as the response of the array with respect to that incident angle. The responses, normalized by the one corresponding to the steering angle, are plotted versus the incident angle to generate the so-called measured beam pattern. For this array, the shape of these beam patterns is very close to the cardioid.

The case  $\bar{\epsilon} = \mu + 3\sigma$  corresponds to the worst-case performance optimization.<sup>11</sup> With the decrease of  $\bar{\epsilon}$ , the directivity rises. This is consistent with Fig. 2(a). The analysis shows that the optimum is around  $\bar{\epsilon} = \mu$ . However, the obtained beam pattern seems more attractive for the case of  $\bar{\epsilon} = \mu - \sigma$ . This does not contradict our previous analysis, as it comes at a cost of an obvious reduction in WNG, which will be discussed in the sequel.

In Fig. 2(b) the estimated values of the DI versus the WNG, for different values of  $\bar{\epsilon}$  are provided. Recall that the DI is defined in the 2D case as

Table 1. Probabilities of  $\gamma \geq 1$  for different values of the regularization parameter  $\bar{\epsilon}$ .

$\bar{\epsilon}$	$\mu - \sigma$	$\mu$	$\mu + \sigma$	$\mu + 3\sigma$
$p$	43%	79%	96%	100%

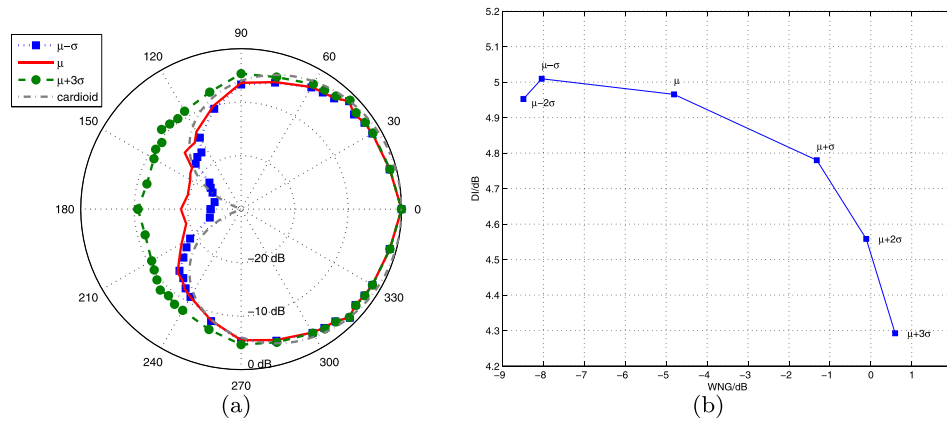


Fig. 2. (Color Online) (a) Beam patterns for different regularization parameters. (b) DI versus WNG for different values of the regularization parameter  $\bar{\epsilon}$ ; for each point, the value of  $\bar{\epsilon}$  is indicated next to the square marker.

$$DI = -10 \log_{10} \left[ \frac{1}{2\pi} \int_0^{2\pi} |\mathcal{B}(\phi)|^2 d\phi \right]. \quad (6)$$

The integration in Eq. (6) is approximated in the present work by the summation over the discrete incident angles. Therefore, these estimates are not very accurate because the gaps between the incident angles are  $5^\circ$  and on most occasions  $15^\circ$ . The definition of the WNG, widely used to measure the robustness of a beamformer, is given by

$$WNG = 10 \log_{10} \frac{|\mathbf{w}^H \mathbf{a}|^2}{\mathbf{w}^H \mathbf{w}}.$$

In Fig. 2(b), the tradeoff relation between DI and WNG is fairly obvious. We can also observe a clear increasing trend of WNG with  $\bar{\epsilon}$ . However, for this sensor array, when the regularization parameter reaches  $\bar{\epsilon} = \mu - \sigma$ , further reducing it brings no benefit; it only reduces the level of robustness without improving the directivity. This can be seen by comparing the two cases  $\bar{\epsilon} = \mu - \sigma$  and  $\bar{\epsilon} = \mu - 2\sigma$ , where the DIs both read 5.0 dB. This figure also shows an increase in the DI of about 0.7 dB when using the PR with  $\bar{\epsilon} = \mu$ , in contrast to the worst-case performance optimization (i.e., PR with  $\bar{\epsilon} = \mu + 3\sigma$ ); this directivity gain comes at a cost of reduced robustness.

The proposed PR method is then compared with two other adaptive beamformers, i.e., the midway method<sup>10</sup> and the WNG constrained regularization,<sup>8</sup> namely “WNC.” The results are shown in Fig. 3. Since there is no clear rule on how to choose an appropriate WNG constraint, we simply set it to 0 dB for the WNC, obtaining one beam pattern. For the PR, the regularization parameter is set to  $\bar{\epsilon} = \mu$ . The obtained beam patterns for the WNC and the PR are almost the same, with approximately identical (measured) DIs of 4.9 and 5.0 dB, respectively. By contrast, the midway offers a mild DI of 3.4 dB. The result of the delay-and-sum (DAS) beamformer, known to be highly robust against the sensor mismatches, is also presented for comparison purposes; it yields a poor DI of only 1.0 dB (measured).

#### 4. Conclusions

In this letter, a robust beamforming method with PR is proposed. This method targets higher directivity compared to other similar robust adaptive approaches while ensuring robustness against the sensor mismatches with a certain probability. The PR problem is solved through the SOC programming with several educated guesses of the regularization parameter  $\bar{\epsilon}$ , which regulates the tradeoff between directivity and robustness. These guesses are tested in MC simulations to determine the optimal regularization parameter; the corresponding beamformer weights provide the solution to the PR problem. Experiments on a  $3 \times 3$  miniaturized URA without calibration were carried out to verify the robustness of the proposed method to sensor mismatches; comparisons with other similar adaptive robust beamformers were also performed.

It is worth mentioning that, during these experiments, the optimum regularization parameter  $\bar{\epsilon}$  was chosen in the range  $\mu \leq \bar{\epsilon} \leq \mu + \sigma$  to ensure robustness with a probability between 79% and 96%, where  $\mu$  and  $\sigma$  are the mean and standard deviation of the possible array manifold distortions. We noticed that this relation between the range  $\mu \leq \bar{\epsilon} \leq \mu + \sigma$  and the probability  $79\% \leq p \leq 96\%$  is least dependent on the exact

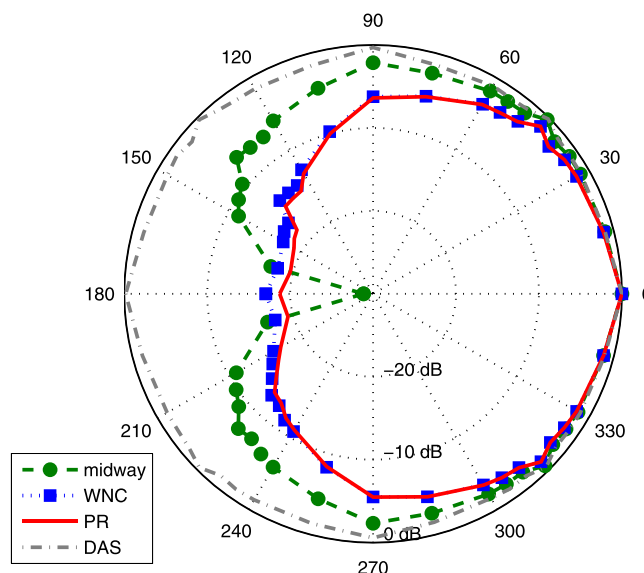


Fig. 3. (Color Online) Comparison of the beam patterns obtained via different beamforming methods.

values of  $\mu$  and  $\sigma$ . Thus, we conjecture that, in general, to meet similar robustness probability requirements, the optimum  $\bar{\varepsilon}$  should also be chosen in the range  $\mu \leq \bar{\varepsilon} \leq \mu + \sigma$  regardless of the exact array geometry and perturbation nature.

### Acknowledgments

This work was supported by the National Natural Science Foundation of China (Grant Nos. 11304251, 11527809, and 51679204) and the Specialized Research Fund for the Doctoral Program of Higher Education of China (Grant No. 20136102120014). The authors would like to thank the anonymous reviewers for their constructive comments and useful suggestions.

### References and links

- <sup>1</sup>J. Chen, J. Benesty, and C. Pan, "On the design and implementation of linear differential microphone arrays," *J. Acoust. Soc. Am.* **136**(6), 3097–3113 (2014).
- <sup>2</sup>C. Pan, J. Benesty, and J. Chen, "Design of robust differential microphone arrays with orthogonal polynomials," *J. Acoust. Soc. Am.* **138**(2), 1079–1089 (2015).
- <sup>3</sup>Y. Wang, Y. Yang, Y. Ma, and Z. He, "Robust high-order superdirectivity of circular sensor arrays," *J. Acoust. Soc. Am.* **136**(4), 1712–1724 (2014).
- <sup>4</sup>S. Doclo and M. Moonen, "Design of broadband beamformers robust against gain and phase errors in the microphone array characteristics," *IEEE Trans. Signal Process.* **51**(10), 2511–2526 (2003).
- <sup>5</sup>H. Chen and W. Ser, "Design of robust broadband beamformers with passband shaping characteristics using Tikhonov regularization," *IEEE Trans. Audio, Speech, Language Process.* **17**(4), 665–681 (2009).
- <sup>6</sup>M. R. Bai and C.-C. Chen, "Regularization using Monte Carlo simulation to make optimal beamformers robust to system perturbations," *J. Acoust. Soc. Am.* **135**(5), 2808–2820 (2014).
- <sup>7</sup>H. Cox, R. M. Zeskind, and M. M. Owen, "Robust adaptive beamforming," *IEEE Trans. Acoust., Speech, Signal Process.* **35**(10), 1365–1376 (1987).
- <sup>8</sup>S. Yan and Y. Ma, "Robust supergain beamforming for circular array via second-order cone programming," *Appl. Acoust.* **66**(9), 1018–1032 (2005).
- <sup>9</sup>L. Du, J. Li, and P. Stoica, "Fully automatic computation of diagonal loading levels for robust adaptive beamforming," *IEEE Trans. Aerosp. Electron. Syst.* **46**(1), 449–458 (2010).
- <sup>10</sup>P. Stoica, J. Li, and X. Tan, "On spatial power spectrum and signal estimation using the Pisarenko framework," *IEEE Trans. Signal Process.* **56**(10), 5109–5119 (2008).
- <sup>11</sup>S. A. Vorobyov, A. B. Gershman, and Z.-Q. Luo, "Robust adaptive beamforming using worst-case performance optimization: A solution to the signal mismatch problem," *IEEE Trans. Signal Process.* **51**(2), 313–324 (2003).
- <sup>12</sup>M. Grant and S. Boyd, "CVX: Matlab software for disciplined convex programming, version 2.1," <http://cvxr.com/cvx>, March 2014 (Last viewed June 10, 2015).